0013-7227/08/$15.00/0
Printed in U.S.A.

Endocrinology 149(8):3989–4000

doi: 10.1210/en.2008-0350

Thyroid Hormone Action in the Adult Brain: Gene Expression Profiling of the Effects of Single and Multiple Doses of Triiodo-L-Thyronine in the Rat Striatum

Diego Diez, Carmen Grijota-Martinez, Patrizia Agretti, Giuseppina De Marco, Massimo Tonacchera, Aldo Pinchera, Gabriella Morreale de Escobar, Juan Bernal, and Beatriz Morte

Instituto de Investigaciones Biomédicas (D.D., C.G.-M., G.M.d.E., J.B., B.M.), Consejo Superior de Investigaciones Científicas and Universidad Autónoma de Madrid (CSIC-UAM), and Centro de Investigación Biomédica en Red de Enfermedades Raras (CIBERER) (C.G.-M., G.M.d.E., J.B., B.M.), Instituto de Salud Carlos III, 28029 Madrid, Spain; and Department of Endocrinology and Metabolism (P.A., G.D.M., M.T., A.P.), Centro Eccellenza AmbiSEN, University of Pisa, 56124 Pisa, Italy

Thyroid hormones have profound effects on mood and behavior, but the molecular basis of thyroid hormone action in the adult brain is relatively unknown. In particular, few thyroid hormone-dependent genes have been identified in the adult brain despite extensive work carried out on the developing brain. In this work we performed global analysis of gene expression in the adult rat striatum in search for genomic changes taking place after administration of T_3 to hypothyroid rats. The hormone was administered in two different schedules: 1) a single, large dose of 25 μg per 100 g body weight (SD) or 2) 1.5 μg per 100 g body weight once daily for 5 d (RD). Twenty-four hours after the single or last of multiple doses, gene expression in the striatum was analyzed using Codelink microarrays. SD caused up-regulation of 149 genes and down-regulation of 88 genes. RD caused up-regulation of 18 genes and down-regulation of one gene. The results were confirmed by hybridization to Affymetrix microarrays and by TaqMan PCR. Among the genes identified are genes involved in circadian regulation and the regulation of signaling pathways in the striatum. These results suggest that thyroid hormone is involved in regulation of striatal physiology at multiple control points. In addition, they may explain the beneficial effects of large doses of thyroid hormone in bipolar disorders. (*Endocrinology* 149: 3989–4000, 2008)

THE EFFECTS AND mechanisms of action of thyroid hormone on the developing brain have been extensively studied (1, 2). Thyroid hormone has multiple actions on brain maturation, resulting from regulation of neural cell migration and differentiation, synaptogenesis, and myelination. Hypothyroidism alters neuronal migration in the cerebral cortex and the cerebellum and impairs the differentiation of pyramidal cells, Purkinje cells, γ-aminobutyric acid (GABA)ergic cell precursors, oligodendrocytes, astrocytes, and microglia. Most if not all of these actions of thyroid hormone are due to regulation of gene expression mediated by interaction with transcriptionally active nuclear receptors (3).

The molecular basis of thyroid hormone action in the mature brain is less well known, despite its importance in brain function. In adults thyroid hormone influences mood and behavior, and thyroid dysfunction very often leads to psychiatric disorders (4). High doses of T_4 are effective in bipolar depression (5, 6). Despite these observations, very little is known on the mechanisms of action of thyroid hormone in the adult brain. Neurotransmitter systems are affected by deficiency or excess of thyroid hormones (7), and thyroid hormone influences neurogenesis in the subventricular and subgranular zones in the adult rat brain (8, 9). Thyroid hormone receptors are widely expressed in the adult brain, and particularly the TRα1 isoform has been implicated in the control of pathways regulating behavior (10). As in other tissues, it is most likely that the action of thyroid hormone in the adult brain is exerted through the control of gene expression. However, an important feature of thyroid hormone action is that the genes regulated by thyroid hormones in the developing brain are insensitive to thyroid hormone in the adult brain, with some exceptions (2).

The purpose of the present work was to fill an important gap in our knowledge of thyroid hormone action in the adult brain by the identification of thyroid hormone-responsive genes. For this study we selected the striatum for two main reasons. One reason was because the thyroid hormone regulated gene *Nrgn* (also known as RC3), is responsive to T_3 in the striatum but not other regions of the adult brain (11). Another reason was the problems of sensitivity threshold due to the high complexity of the whole brain: the cellular complexity of the striatum is not as high as other regions of potential interest such as the cerebral cortex because a single cell type, the GABAergic medium-spiny projection neuron, represents more than 90% of the total cell population. It is worth mentioning in this context that the striatum was one of the regions showing altered metabolic activity after administration of T_4 to bipolar patients (6).

We analyzed the effects of single and multiple doses of T_3

First Published Online May 8, 2008

Abbreviations: DARPP, Dopamine and cAMP-regulated phosphoprotein; D1, type 1 deiodinase; GABA, γ-aminobutyric acid; GO, gene ontology; P, postnatal day; RD, repeated doses; SD, single dose; SNR, signal to noise ratio; TX, hypothyroid rats.

***Endocrinology* is published monthly by The Endocrine Society (http://www.endo-society.org), the foremost professional society serving the endocrine community.**

administration to hypothyroid rats on striatal gene expression by microarray analysis. As a result, we identified novel gene targets of thyroid hormone. In terms of gene regulation, the effect of a single, large dose of T_3 was more dramatic than that of multiple lower doses, probably indicating that amplified gene responses to T_3, as occurs in liver (12), are also present in the adult brain. This observation is important to explain the beneficial effects of large doses of thyroid hormone in bipolar disorders.

Materials and Methods

Animals and treatment

Rats from the Wistar strain grown in our animal facilities were used. Protocols for animal handling were approved by the local institutional Animal Care Committee and followed the rules of the European Union. Animals were under temperature (22 ± 2 C) and light (12-h light, 12-h dark cycle; lights on at 0700 h) controlled conditions and had free access to food and water. Hypothyroidism was induced in adult male rats at postnatal day (P) 50 by surgical thyroidectomy, taking care to spare the parathyroid glands (9). To ensure complete thyroidectomy, the rats were given the antithyroid compound 2-mercapto-1-methylimidazole (Sigma Chemical Co., St. Louis, MO) 0.02% in the drinking water until the end of the experiment, on P75. Hypothyroid rats (referred to as TX) had low serum levels of both T_4 (0.34 ± 0.13 ng/ml) and T_3 (0.07 ± 0.05 ng/ml), compared with normal rats of the same age (24.8 ± 5.7 and 0.49 ± 0.07 ng/ml, respectively). Serum thyroid hormones were measured as described (13).

T_3 (Sigma), dissolved in 0.05 M NaOH and diluted in saline containing 0.1% BSA, was administered ip to the TX rats according to two different schedules: in one group T_3 was given as a single dose of 25 μg of T_3 per 100 g body weight on P74, *i.e.* 24 h before the animals were killed (SD group). Plasma T_3 concentration 24 h after the injection was 4.35 ± 1.93 ng/ml, corresponding to an estimated fractional occupancy of T_3 nuclear receptors of 0.87, according to the formula: occupancy = plasma T_3/(plasma T_3 + 0.67) (14). The SD group was used to identify fast changes of gene expression taking place after T_3 administration to TX rats, under conditions of near full saturation of nuclear receptors for 24 h. A second group of TX rats was also treated with T_3 but for 5 d with single daily doses of 1.5 μg of T_3 per 100 g body weight, starting on P70 (RD group). Plasma T_3 concentration 24 h after the last injection was 0.66 ± 0.17 ng/ml and an estimated T_3 receptor occupancy of 0.49. The effect of T_3 treatment was monitored by Northern blotting analysis of liver type 1 deiodinase (D1) mRNA (15) and quantified by densitometry using the National Institutes of Health Image J software (http://rsb.info.nih.gov/ij/), with correction for the housekeeping gene *Gapdh*. Both treatment schedules resulted in similar inductions of D1 mRNA (TX: 0.40 ± 0.05; SD: 1.30 ± 0.20; RD: 1.15 ± 0.20, $P < 0.05$ for T_3 treated *vs.* TX).

The animals, weighing about 200 g, were killed by decapitation under anesthesia with a mixture of ketamine and medetomidine (9) 24 h after the single T_3 dose or the last of the multiple doses. The brain was rapidly removed and the striatum was isolated after separation from the internal capsule and kept frozen at −80 C until RNA preparation.

RNA analysis

Total RNA was isolated individually from each animal using the Trizol procedure (Invitrogen, Carlsbad, CA), with an additional step of chloroform extraction. The quality of RNA was analyzed using a Bio-Analyzer (Agilent, Santa Clara, CA). cDNA was prepared from 250 ng of RNA using the high-capacity cDNA reverse transcription kit (Applied Biosystems, Foster City, CA). For quantitative PCR, a cDNA aliquot corresponding to 5 ng of the starting RNA was used, with Taqman Assay-on-Demand primers and the Taqman universal PCR master mix, No Amp Erase UNG (Applied Biosystems) on a 7900HT fast real-time PCR system (Applied Biosystems). The PCR program consisted in a hot start of 95 C for 10 min, followed by 40 cycles of 15 sec at 95 C and 1 min at 60 C. PCRs were performed in triplicates, using the 18S gene as internal standard and the 2-cycle threshold method for analysis (16).

Individual striatal RNA samples from six hypothyroid, four SD, and five RD rats were hybridized to separate Codelink microarrays (rat whole genome bioarray; GE Healthcare Europe GmbH, Munich, Germany). These arrays contain 33,849 probes, representing 14,519 unique sequences. A limited survey was also performed using RNA pools from five animals of each condition and hybridized to the Rat Expression Array 230A (product 511036 from Affymetrix, Santa Clara, CA), containing 10,417 unique sequences. There were 9749 sequences common to both platforms (see supplemental Fig. 1, published as supplemental data on The Endocrine Society's Journals Online web site at http://endo.endojournals.org). All procedures were as recommended by the manufacturers. Codelink hybridizations were performed at the Instituto de Investigaciones Biomédicas, Madrid, whereas Affymetrix hybridizations were performed at the University of Pisa.

Analysis of the data from microarray hybridizations

The data were analyzed using the *R* software (17) and packages from the Bioconductor project (http://www.bioconductor.org/) (18, 19). The *codelink* (20) and *affy* (21) packages were used for reading and preprocessing the arrays, *genefilter* (22) for data filtering and *limma* (23) for statistical analysis. For Codelink arrays, raw intensities were exported for each array with the Codelink software and the files read into *R*. Background correction using the *normexp* method and *quantile* normalization was applied. Probes having a signal to noise ratio (SNR) below 1 in all samples were removed from further analysis. Gene-wise intensities were fitted to a linear model with the experimental group (TX, RD, and SD) as factor and contrasts RD-TX and SD-TX were computed to identify genes differentially expressed between the treatments and the reference group. Genes were selected as differentially expressed with $P_{adjust} < 0.05$ (24). Data from the Affymetrix arrays were loaded into *R* and processed using the robust multichip average (25) method. Genes were selected based on fold change to compare the results with the Codelink data. For this task an absolute fold change of 1.6 was used. (0.7 in $\log_2$ scale).

We performed an analysis of enriched gene ontology (GO) (26) categories to look for affected biological processes, molecular functions, or pathways using the PANTHER resource (27). A gene universe was created by filtering from the list of all probes in the array those not expressed, *i.e.* with a SNR less than 1 in all samples. After that, we translated the probe identifiers to Entrez Gene identifiers (removing any probe without Entrez Gene) and filtered those lacking GO annotations. Finally, we removed all duplicated Entrez Gene identifications, obtaining 7,287 identifiers from the original 33,849 probes (supplemental Table 1. For the test we translated the list of differentially expressed genes to Entrez Gene and removed those not present in the universe.

FIG. 1. Effects of T_3 on gene expression in the adult rat striatum. A, Two-dimensional representation of expression values (heat map) across all samples and differentially expressed genes. All intensities were normalized across the rows (subtracting the mean and dividing by the SD) to enable comparison between genes. The normalized log intensity values of the probes were centered to the median value of each probe set and colored on a range of +2 (*red*) and −2 (*blue*); *yellow* indicates intermediate value. *Columns* correspond to samples, whereas *row* corresponds to individual probe sets (in some cases several probe sets correspond to the same gene). Two main clusters, a and b, classify the differentially expressed genes as having higher or lower expression after T_3 treatment, respectively. The *horizontal arrow* shows a cluster of genes showing higher expression after multiple doses of T_3 (RD group) but not after a single dose (SD group). B, The profiles plot shown here contains the same information found in the heat map but with a different perspective. This allows us to focus on the general tendency of selected gene clusters. Signal intensities are normalized as in the heat map and expression values and colored based on the overall pattern. For each pattern, a loess (locally weighted polynomial regression) fit line describes the overall profile of the corresponding group. This tendency profile is plotted

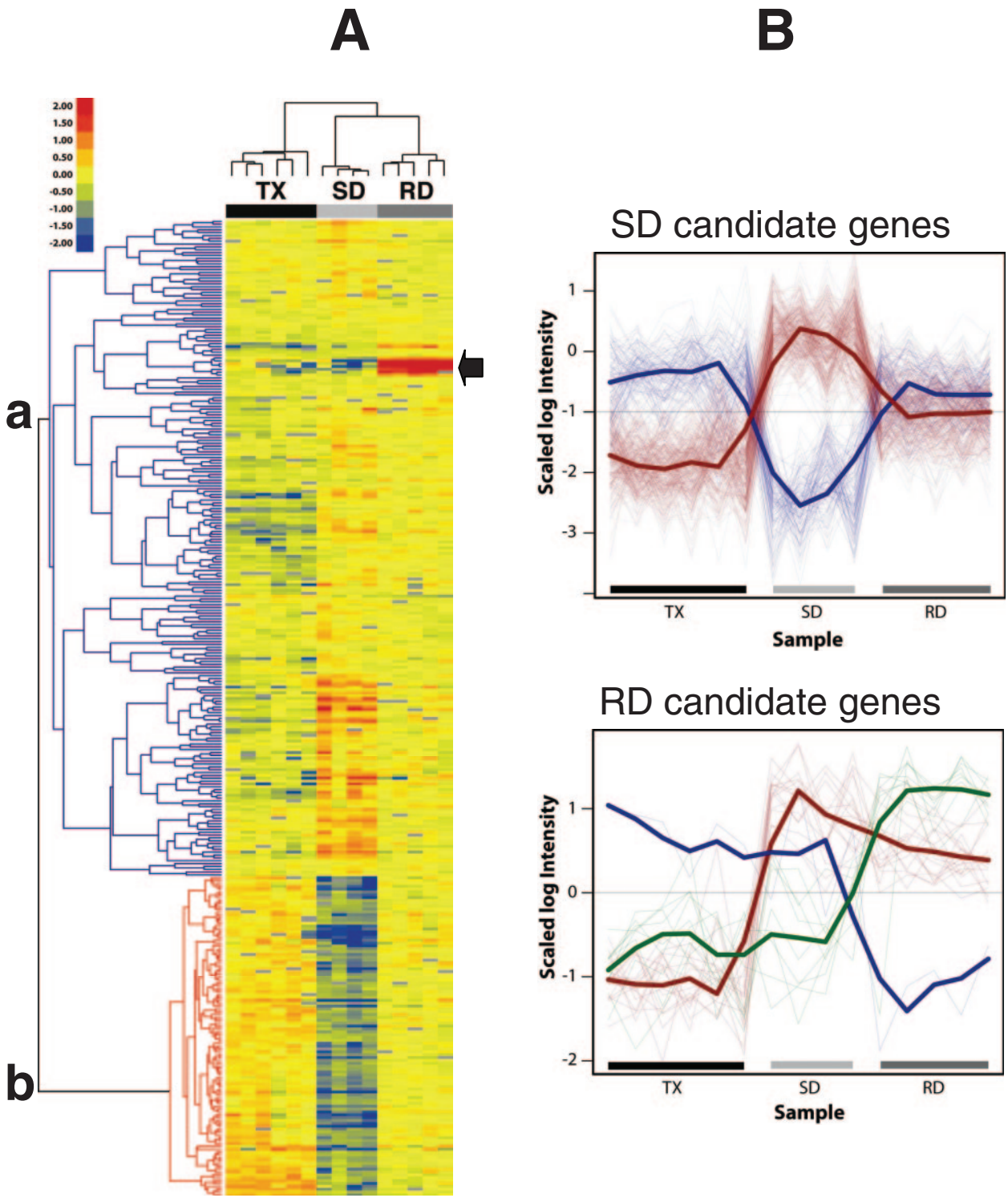

separately for genes up-regulated (*red* and *green*) and down-regulated (*blue*). The *upper panel* shows the expression values of each of the 222 up-regulated sequences and 112 down-regulated sequences selected after the T_3 single dose (SD group) in the individual arrays for the three experimental groups. The *lower panel* corresponds to the expression values of each of the 25 up-regulated sequences and the one that was down-regulated after the T_3 repeated dose (RD group). In the RD group, the up-regulated genes follow two trends: one with little change in the SD group (*green line*) and another that was also changed in the SD group (*red line*); there was only one gene decreased after RD (*blue line*). Most of the genes in cluster a of the heat map correspond to genes following the *blue line* in B. On the other hand, genes in cluster b in the heat map correspond to genes following the *red line* in B. Those genes indicated with the *green line* correspond to the cluster shown with an *arrow* in the heat map.

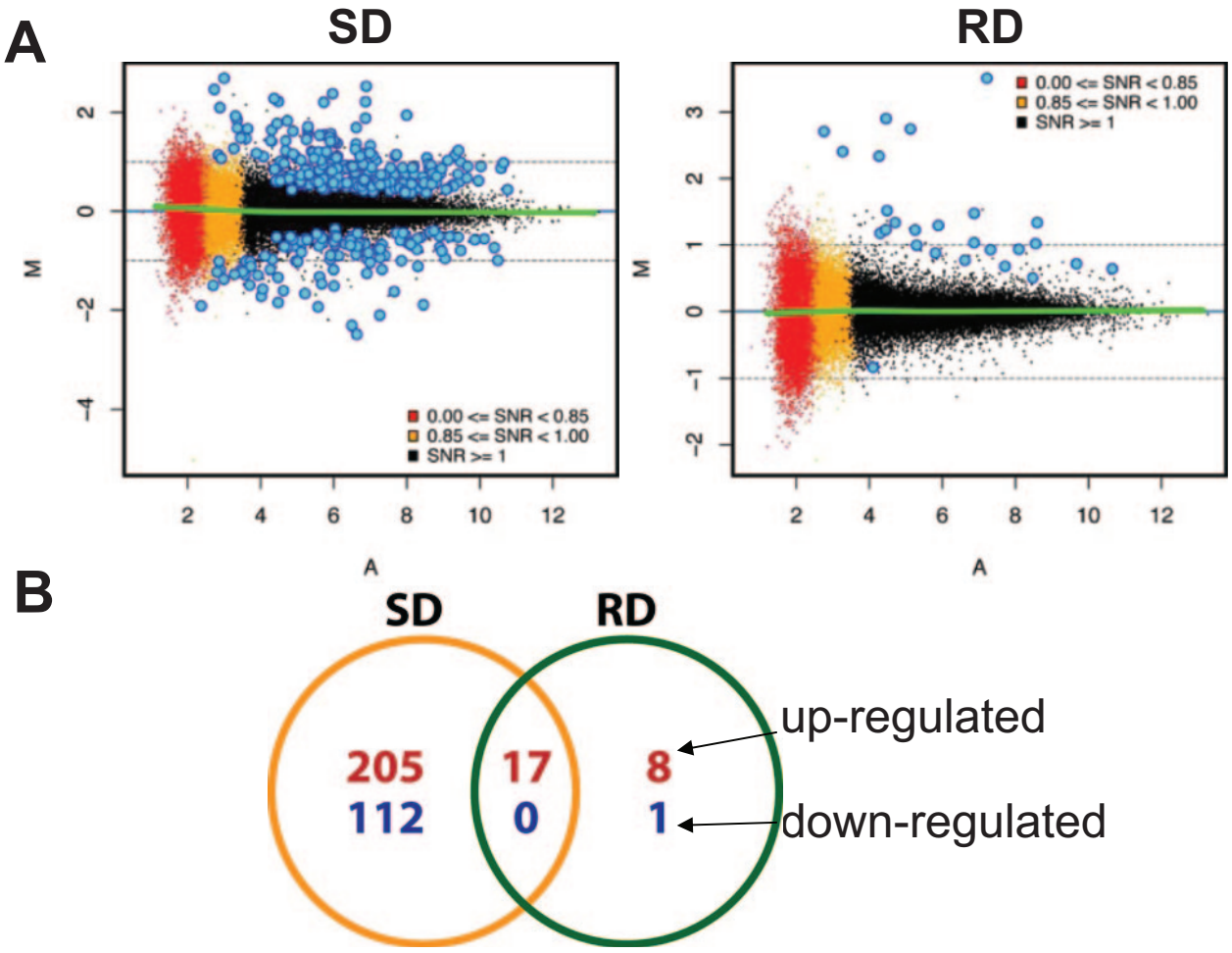

FIG. 2. Effects of single (SD) and multiple (RD) doses of T_3 on gene expression after administration to TX animals. A, MA plots, relating the $\log_2$ of the fold change (M, in ordinate) *vs.* the mean of log intensity of the signal (A, in abscissa) of SD *vs.* TX and RD *vs.* TX. *Red* and *orange dots* represent probe sets having SNRs of 1 or below. *Black dots* are probe sets with SNR above 1. The *blue dots* represent the differentially expressed sequences, with $P_{adjust} < 0.05$. B, Venn diagram showing the quantitative relation between the number of sequences differentially expressed in the SD and RD groups.

Results

Effects of T_3 on gene expression in the adult striatum

To analyze the effects of thyroid hormone on gene expression in the adult rat striatum, T_3 was administered to hypothyroid rats either acutely (SD) or as single daily doses (RD). RNA from individual rat striata was used to hybridize Codelink microarrays. Both the SD and RD treatments resulted in changes of gene expression. Figure 1A shows the hierarchical clustering (heat map) of all the individual data representing the differentially expressed sequences at a significance level of $P_{adjust} < 0.05$. The complete, annotated heat map is shown as supplemental Fig. 2. The columns contain the data from individual samples, which clustered in three groups as a function of treatment. The rows show the relative intensity of the probes, centered around the mean intensity for all individual RNAs. The probes were grouped in two main clusters: one group (cluster a) contained sequences whose expression increased after T_3. The second group (cluster b) contained sequences whose expression was decreased by T_3. Visual inspection of the heat map also revealed that the effect of the SD was more pronounced than the RD, although in most cases there was also an effect but of lower intensity of the RD.

The comparisons between the effects of the SD *vs.* the RD are clearly seen in the plot profiles shown in Fig. 1B. These plots show the expression values along different arrays for the probes selected as differentially expressed in the two treatment groups. The signal intensities are scaled to the same range so that they can be compared. The tendency profile [Loess curve (28)] is plotted separately for up-regulated (Fig. 1B, *red* and *green*) and down-regulated (Fig. 1B, *blue*) genes. The *upper panel* shows the behavior in each group of the genes that changed after the single T_3 dose (SD group). The *lower panel* shows the genes whose expression was changed after the multiple T_3 doses (RD group). The data indicate that administration of a single high dose of T_3 sets in motion large changes of gene expression, in contrast to the more discrete changes after treatment with the much lower, multiple doses.

Figure 2 shows the MA scatter plots (Fig. 2, *upper panels*) and the Venn diagram (Fig. 2, *lower panel*). The MA plots relate the $\log_2$ of the fold change (M) of the signal after T_3

treatment with its mean log-expression level (A) in the treated and untreated groups. The *dotted horizontal lines* represent a fold change of 2 for up-regulated genes or 50% for down-regulated genes. The *blue dots* represent the differentially expressed probe sets with $P_{adjust} < 0.05$. In the SD group, 334 sequences were differentially expressed with respect to the hypothyroid animals. From them, 222 sequences were up-regulated and 112 sequences down-regulated. After subtracting 80 nonannotated sequences and 17 repeated probes, there were 149 up-regulated and 88 down-regulated genes. Many of the statistically significant, differentially expressed genes had absolute M values as low as 0.5, indicating moderate changes of gene expression. After filtering the data on the basis of fold change, there were 91 up-regulated genes and 53 down-regulated genes with absolute M values greater than 0.7.

The RD caused changes of expression of 26 sequences. After subtracting the nonannotated and repeated sequences, 18 genes were up-regulated and one was down-regulated [*Gja7*, or connexin 45 (29)]. As shown in the intersection between the SD and RD in the Venn diagram, 17 sequences were up-regulated with both treatment schedules. This set of 17 sequences corresponded to 10 unique genes: the cannabinoid receptor *Cnr1*, an important G protein-coupled receptor (30), recently linked to hyperactivity of neonatal hypothyroid rats (31); angiotensin converting enzyme, *Ace*, a component of brain renin-angiotensin system (32); the sonic hedgehog transcriptional effector *Gli1*, linked to neuroprotection in the adult brain (33); the sonic hedgehog responsive gene *Ith3* [inter-α trypsin inhibitor (34)]; the extraneuronal monoamine transporter *Slc22a3*, implicated in several neurological disorders (35); the voltage gated sodium channel β4-subunit, *Scn4b*, involved in electrical signaling and cell adhesion and defective in Huntington's disease (36, 37); the small heat shock protein *Hspb6* (38); *Grifin*, or galactin-related interfiber protein originally described in the lens (39); and *Loc290651*, similar to myoinositol 1-phosphate synthase A1, and *RGD1305038_predicted*, similar to serum-inducible kinase.

The mean expression of the eight sequences specifically increased by RD with $P < 0.05$ is represented as a *green line* in the plot profile of Fig. 1B. Seven of these sequences could be observed as a prominent cluster in the heat map (Fig. 1, *horizontal arrow*). Three of these genes are related to red blood cells (*Loc287167*, *Hba1*, and *AlaS2*); *Ceacam1* encodes a cell adhesion molecule (40); *Prph1* encodes the intermediate filament and Akt substrate peripherin (41, 42); and *Cd52* encodes a surface antigen.

The complete set of genes that were differentially expressed in the SD and RD groups, selected on the basis of statistical significance is shown as supplemental Table 2. From these data, genes having a fold change of at least 1.6 in any of the two treatment groups are displayed in Table 1. This table shows the fold change in the SD and the RD groups and the A value. The A value corresponds to the mean of the log2 intensity values over all samples and is a measure of the average expression level. Values with $P_{adjust} < 0.05$ are highlighted. The genes were categorized according to the biological processes or molecular function assigned by GO annotation (26). The GO annotation suggested that the differentially expressed genes were involved in a variety of biological processes.

To determine the statistical significance of these observations, we used PANTHER analysis to identify those categories significantly over- or downrepresented within the group of differentially expressed genes in relation to the universe of expressed genes in the striatum as found in the arrays (7287; see *Materials and Methods*). The analysis (supplemental Table 3) showed the pathway, biological process and molecular function categories with over- or downrepresented candidate genes with $P < 0.05$. Within the pathway category, we found three genes related to the circadian clock system (*Per1*, *Per2*, *Nr1d2*); heterotrimeric G protein signaling pathways (Gqα and Goα-mediated pathways: *Rgs2*, *Rgs14*, *Rgs9*, *Rasgrp1*, *Arhgef3_predicted*, *Rhoc_predicted*, *Rap1ga1*, *Rasgrp2_predicted*); oxidative stress response (*Dusp1*, *Dusp5*, *Map2k3*, *Dupd1_predicted*); phenylethylamine degradation (*Aldh1a1*, *Doxl1*); and MAPK pathway (*Map2k3*, *Fos*, *Rps6ka4_predicted*). Within the biological process and molecular function categories, we found, among others, genes involved in regulation of phosphate metabolism, signal transduction, tyrosine kinase signaling pathways, extracellular transport and import, cell structure, and neuronal activity.

Confirmation of microarray data

We used two approaches to confirm the data. First, we checked the reproducibility of the assay in a different platform. Reproducibility of microarray data across different platforms and laboratories is dramatically dependent on the criteria used to select the differentially expressed genes (43). In our studies we analyzed individual RNAs and applied the *limma* statistics to account for variability of the data and therefore selected the candidate genes on the basis of adjusted *P* value. On the other hand, it has been noted that selection on the basis on fold change achieves better reproducibility among different platforms and biological groups than a selection based on *t* statistics (44, 45).

Therefore, as a secondary screening for partial validation of the data and to select sequences for further confirmation by PCR, we performed an independent analysis using the Affymetrix platform. In this assay, we used pools of RNA instead of individual samples. Striatal RNA from five animals of each group were pooled and hybridized to the Affymetrix rat expression arrays 230A. Candidate genes were selected on the basis of an increase or decrease of at least 1.6-fold and compared with the candidate genes previously selected from the Codelink arrays. These comparisons were limited by the fact that some genes were uniquely present in one of the two different arrays (see supplemental Fig. 1 and supplemental Table 4). Fifty two differentially expressed genes from the Codelink platform were absent from the Affymetrix arrays, and 20 genes with an M value above 0.7 in the Affymetrix arrays were absent from the Codelink arrays. Among the latter, *Nrgn* and *Tubb3*, known to be dependent of the thyroid status (11, 46), were found as induced by SD and RD treatments in the Affymetrix arrays (not shown) but were not present as probes in the Codelink arrays.

TABLE 1. Differentially expressed genes grouped by biological process (BP; GO)

Entrezid	Symbol	Name	SD	RD	A
BP: regulation of transcription, DNA dependent					
140589	Gli1	GLI-Kruppel family member GLI1	**3.43**	**2.35**	4.45
306873	Rreb1_predicted	Ras responsive element binding protein 1 (predicted)	**2.91**	1.13	5.62
24309	Dbp	D site albumin promoter binding protein	**2.66**	−1.07	5.91
60563	hr	Hairless homolog (mouse)	**2.64**	1.00	6.02
298894	Mycn	V-myc myelocytomatosis viral related oncogene, neuroblastoma derived (avian) (mapped)	**2.30**	1.17	5.44
313575	Heyl_predicted	Hairy/enhancer-of-split related with YRPW motif-like (predicted)	**2.23**	1.49	4.89
24309	Dbp	D site albumin promoter binding protein	**2.00**	1.13	9.47
361715	Rps6ka4_predicted	Ribosomal protein S6 kinase, polypeptide 4 (predicted)	**1.93**	1.25	5.91
117560	Klf9	Kruppel-like factor 9	**1.91**	1.55	8.67
117560	Klf9	Kruppel-like factor 9	**1.83**	1.48	10.58
308435	Cic_predicted	Capicua homolog (Drosophila) (predicted)	**1.67**	1.20	8.21
497984	RGD1566329 predicted	Similar to zinc finger protein 652 (predicted)	−1.13	**6.73**	5.13
287422	Per1	Period homolog 1 (Drosophila)	**−1.83**	−1.23	6.61
24330	Egr1	Early growth response 1	**−1.99**	−1.02	10.5
25129	Egr4	Early growth response 4	**−2.16**	1.13	8.31
114519	Nfil3	Nuclear factor, IL-3 regulated	**−2.27**	−1.06	6.01
304741	Tcfcp2l1_predicted	Transcription factor CP2-like 1 (predicted)	**−2.35**	−1.13	2.81
314322	Fos	FBJ murine osteosarcoma viral oncogene homolog	**−3.07**	−1.16	7.66
79240	Nr4a1	Nuclear receptor subfamily 4, group A, member 1	**−3.71**	−1.16	8.46
58853	Nr4a3	Nuclear receptor subfamily 4, group A, member 3	**−3.81**	−1.12	5.57
58853	Nr4a3	Nuclear receptor subfamily 4, group A, member 3	**−4.29**	−1.03	7.26
114090	Egr2	Early growth response 2	**−4.96**	−1.07	6.51
29546	Homer1	Homer homolog 1 (Drosophila)	**−5.58**	−1.30	6.64
BP: intracellular signaling cascade					
64032	Ctgf	Connective tissue growth factor	**2.99**	1.64	5.3
60669	Cmklr1	Chemokine-like receptor 1	**2.31**	1.22	5.81
25248	Cnr1	Cannabinoid receptor 1 (brain)	**2.11**	**2.03**	8.55
361715	Rps6ka4_predicted	Ribosomal protein S6 kinase, polypeptide 4 (predicted)	**1.93**	1.25	5.91
311118	Tlk1_predicted	Tousled-like kinase 1 (predicted)	**−1.64**	−1.11	4.91
114108	Pdlim3	PDZ and LIM domain 3	**−1.80**	1.11	6.89
24716	Ret	Ret protooncogene	**−1.87**	−1.60	4.12
29546	Homer1	Homer homolog 1 (Drosophila)	**−5.58**	−1.30	6.64
Small GTPase-mediated signal transduction					
306873	Rreb1_predicted	Ras responsive element binding protein 1 (predicted)	**2.91**	1.13	5.62
310838	Bcar3_predicted	Breast cancer antiestrogen resistance 3 (predicted)	**2.57**	1.39	6.61
310838	Bcar3_predicted	Breast cancer antiestrogen resistance 3 (predicted)	**2.39**	1.33	6.61
114203	Aps	Adaptor protein with pleckstrin homology and src homology 2 domains	**2.31**	1.12	5.39
303653	Cdc42ep4_predicted	CDC42 effector protein (ρ GTPase binding) 4 (predicted)	**2.25**	1.19	6.77
303653	Cdc42ep4_predicted	CDC42 effector protein (ρ GTPase binding) 4 (predicted)	**2.23**	1.29	6.84
171099	Rasd2	RASD family, member 2	**1.88**	1.45	10.03
299824	RGD1305255 predicted	Similar to CG3996-PA (predicted)	**1.79**	1.53	5.61
360571	Rab34	RAB34, member of RAS oncogene family	**1.67**	1.15	6.57
192126	Dab2ip	Disabled homolog 2 (Drosophila) interacting protein	**1.65**	1.15	8.78
292750	Plekhg2_predicted	Pleckstrin homology domain containing, family G (with RhoGef domain) member 2 (predicted)	**−1.66**	1.04	6.63
308821	Rab30	RAB30, member RAS oncogene family	**−2.81**	−1.24	3.71
686142	LOC686142	Similar to Ral guanine nucleotide dissociation stimulator (RalGEF) (RalGDS)	**−2.85**	1.13	6.01
G protein-coupled receptor protein signaling pathway					
29481	Rgs9	Regulator of G-protein signaling 9	**2.75**	1.62	5.26
29481	Rgs9	Regulator of G-protein signaling 9	**2.71**	1.78	6.01
84583	Rgs2	Regulator of G-protein signaling 2	**−1.66**	1.09	8.9
Protein tyrosine phosphatase activity					
246781	Ptpn7	Protein tyrosine phosphatase, nonreceptor type 7	**−1.64**	−1.04	6.65
171109	Dusp5	Dual specificity phosphatase 5	**−2.03**	−1.06	5.02
295338	Ptpn22_predicted	Protein tyrosine phosphatase, nonreceptor type 22 (lymphoid) (predicted)	**−1.65**	1.05	4.73
114856	Dusp1	Dual-specificity phosphatase 1	**−2.06**	−1.39	7.01
BP: rhythmic process					
24309	Dbp	D site albumin promoter binding protein	**2.66**	−1.07	5.91
24309	Dbp	D site albumin promoter binding protein	**2.00**	1.13	9.47
287422	Per1	Period homolog 1 (Drosophila)	**−1.83**	−1.23	6.61
29461	Vgf	VGF nerve growth factor inducible	**−1.95**	−1.08	9.05
114090	Egr2	Early growth response 2	**−4.96**	−1.07	6.51
BP: cation transport					
29504	Slc22a3	Solute carrier family 22, member 3	**2.73**	**2.35**	5.26
83500	Slc22a8	Solute carrier family 22 (organic anion transporter), member 8	**2.69**	1.72	4.28

(*Continues*)

TABLE 1. *Cont.*

Entrezid	Symbol	Name	SD	RD	A
29726	Slc22a5	Solute carrier family 22 (organic cation transporter), member 5	**2.16**	1.02	4.96
315611	Scn4b	Sodium channel, voltage-gated, type IV, β	**1.97**	1.56	10.65
315611	Scn4b	Sodium channel, voltage-gated, type IV, β	**1.88**	**1.65**	9.67
170546	Ryr3	Ryanodine receptor 3	**1.84**	1.09	7.56
170546	Ryr3	Ryanodine receptor 3	**1.83**	1.19	6.38
252919	Slc38a3	Solute carrier family 38, member 3	**1.82**	1.13	5.33
170924	Abcc4	ATP-binding cassette, subfamily C (CFTR/MRP), member 4	**1.67**	1.15	4.91
155205	Slc36a1	Solute carrier family 36 (proton/amino acid symporter) member 1	**−2.16**	1.01	3.73
85267	Slc24a3	Solute carrier family 24 (sodium/potassium/calcium exchanger), member 3	**−2.41**	1.00	3.29
BP: cell organization and biogenesis					
315131	Kdelr3_predicted	KDEL (Lys-Asp-Glu-Leu) endoplasmic reticulum protein retention receptor 3 (predicted)	**6.50**	1.52	3.01
63878	Stc2	Stanniocalcin 2	**5.54**	3.41	2.73
25602	Tnxa	Tenascin XA	**5.21**	1.93	5.97
316638	Sned1	Insulin responsive sequence D binding protein-1	**2.93**	1.67	5.76
362650	Fblim1	Filamin binding LIM protein 1	**2.81**	1.96	3.45
171112	Wfdc1	WAP four-disulfide core domain 1	**2.17**	1.27	7.69
29317	Csrp2	Cysteine and glycine-rich protein 2	**2.04**	1.40	7.16
89806	Tie1	Tyrosine kinase with immunoglobulin-like and EGF-like domains 1	**1.91**	1.14	6.48
307235	RGD1311910 predicted	Similar to hypothetical p38 protein (predicted)	**1.88**	−1.08	6.52
85251	Col18a1	Procollagen, type XVIII, α1	**1.80**	1.13	4.39
308345	Suv420h2_predicted	Suppressor of variegation 4–20 homolog 2 (Drosophila) (predicted)	**1.68**	1.22	7.43
360537	Tom1l2_predicted	Target of myb1-like 2 (chicken) (predicted)	**1.68**	1.01	4.85
362584	Col9a2_predicted	Procollagen, type IX, α2 (predicted)	**1.68**	1.13	5.94
81613	Ceacam1	CEA-related cell adhesion molecule 1	1.46	**2.53**	4.71
266706	Gja7	Gap junction membrane channel protein α7	−1.09	**−1.78**	4.11
24688	Prph1	Peripherin 1	−1.10	**1.92**	8.11
362873	Plxnc1_predicted	Plexin C1 (predicted)	**−1.62**	−1.16	5.11
287925	Pkp2	Plakophilin 2	**−1.62**	1.05	5.61
306081	Pcdh20_predicted	Protocadherin 20 (predicted)	**−1.65**	−1.03	7.27
54323	Arc	Activity regulated cytoskeletal-associated protein	**−2.00**	1.15	7.86
306548	Hook3	Hook homolog 3 (Drosophila)	**−2.01**	−1.18	2.86
79110	Mepe	Matrix extracellular phosphoglycoprotein with ASARM motif (bone)	**−2.58**	−1.11	2.99
BP: cellular lipid metabolism					
89826	Rpe65	Retinal pigment epithelium 65	**3.23**	1.61	3.36
89826	Rpe65	Retinal pigment epithelium 65	**2.16**	1.71	4.08
84575	Fads1	Fatty acid desaturase 1	**1.93**	1.47	6.81
117243	Acsl6	Acyl-CoA synthetase long-chain family member 6	**1.82**	1.36	8.95
94338	Smpd3	Sphingomyelin phosphodiesterase 3, neutral	**1.77**	1.28	8.76
170465	Acaa2	Acetyl-coenzyme A acyltransferase 2 (mitochondrial 3-oxoacyl-coenzyme A thiolase)	**1.67**	−1.09	7.39
25702	Pnlip	Pancreatic lipase	1.46	**1.91**	7.32
304741	Tcfcp2l1_predicted	Transcription factor CP2-like 1 (predicted)	**−2.35**	−1.13	2.81
BP: protein metabolism					
24310	Ace	Angiotensin I-converting enzyme (peptidyl-dipeptidase A) 1	**4.66**	**2.79**	6.87
295394	Dph5	DPH5 homolog (S. cerevisiae)	**2.20**	1.35	2.84
25697	Ctsl	Cathepsin L	**1.72**	1.21	5.91
364948	Asphd2	Aspartate β-hydroxylase domain containing 2	**1.69**	1.25	7.67
308345	Suv420h2_predicted	Suppressor of variegation 4–20 homolog 2 (Drosophila) (predicted)	**1.68**	1.22	7.43
300981	Acy1	Aminoacylase 1	**1.67**	1.28	7.66
310467	Tiparp_predicted	TCDD-inducible poly(ADP-ribose) polymerase (predicted)	**−1.85**	−1.16	5.91
303287	Fbxo39	F-box protein 39	**−2.27**	1.20	4.26
29154	Capn2	Calpain 2	**−2.39**	−1.11	6.91
BP: others					
303772	Slc16a6	Solute carrier family 16 (monocarboxylic acid transporters), member 6	**5.78**	2.11	6.89
303772	Slc16a6	Solute carrier family 16 (monocarboxylic acid transporters), member 6	**4.86**	2.25	4.37
303772	Slc16a6	Solute carrier family 16 (monocarboxylic acid transporters), member 6	**4.29**	1.21	2.89
293628	RGD1308955	Similar to Cc1–9	**3.81**	2.04	3.31
314627	RGD1305038 predicted	Similar to serine/threonine-protein kinase SNK (serum inducible kinase) (predicted)	**3.25**	**1.71**	6.62
296048	Agpat7_predicted	1-Acylglycerol-3-phosphate *O*-acyltransferase 7 (lysophosphatidic acid acyltransferase, η) (predicted)	**2.51**	1.71	7.01
192245	Hspb6	Heat shock protein, α-crystaline-related, B6	**2.22**	**1.60**	7.72
50693	Itih3	Inter-α trypsin inhibitor, heavy chain 3	**1.95**	**2.53**	8.61
287437	Tnfsf13	TNF (ligand) superfamily, member 13	**1.91**	1.17	6.31
303601	Cyb561_predicted	Cytochrome b-561 (predicted)	**1.88**	1.39	8.2
54283	Pfkfb4	6-Phosphofructo-2-kinase/fructose-2,6-biphosphatase 4	**1.83**	1.12	6.11
24188	Aldh1a1	Aldehyde dehydrogenase family 1, member A1	**1.67**	1.55	5.33

(*Continues*)

TABLE 1. *Cont.*

Entrezid	Symbol	Name	SD	RD	A
260327	Fndc5	Fibronectin type III domain containing 5	**1.67**	1.29	7.93
293587	RGD1311186 predicted	Similar to RIKEN cD 1810014F10 gene (predicted)	**1.66**	1.30	7.16
303242	DLP2	Dynein-like protein 2	**1.62**	1.13	6.11
25748	Alas2	Aminolevulinic acid synthase 2	1.12	**5.06**	4.27
287167	LOC287167	Globin, α	−1.04	**11.39**	7.22
25632	Hba-a1	Hemoglobin-α, adult chain 1	−1.39	**7.46**	4.46
304017	Tomm70a	Translocase of outer mitochondrial membrane 70 homolog A (yeast)	**−1.66**	−1.02	10.4
25741	Pfkl	Phosphofructokinase, liver, B-type	**−1.97**	−1.02	5.91
171128	Gchfr	GTP cyclohydrolase I feedback regulator	**−2.46**	−1.75	3.93
292686	Fbxo46	F-box protein 46	**−2.77**	1.25	5.67
29625	Crhbp	Corticotropin releasing hormone binding protein	**−3.16**	−1.22	5.21
MF: others					
301073	Gup1_predicted	Gup1, glycerol uptake/transporter homolog (yeast) (predicted)	**4.63**	1.71	5.73
309208	RGD1564983 predicted	Similar to leucine rich repeat containing 10 (predicted)	**3.86**	2.00	8.01
500590	LOC500590	Similar to T cell antigen 4–1BB precursor-mouse	**3.56**	1.16	4.73
117130	Grifin	Galectin-related interfiber protein	**2.41**	**5.31**	3.27
363931	Gtpbp6_predicted	GTP binding protein 6 (putative) (predicted)	**2.19**	1.26	9.32
288689	RGD1566317 predicted	Similar to tescalcin (predicted)	**2.04**	1.44	9.13
63886	Abcb9	ATP-binding cassette, subfamily B (MDR/TAP), member 9	**1.93**	1.45	6.77
367747	RGD1564763 predicted	Similar to nudix (nucleoside diphosphate linked moiety X)-type motif 11 (predicted)	**1.85**	1.38	5.85
361348	RGD1559803 predicted	Similar to maestro (predicted)	**1.73**	1.27	6.59
171451	Mosc2	MOCO sulphurase C-terminal domain containing 2	**1.69**	1.07	8.92
362597	RGD1308876 predicted	Similar to 2610027C15Rik protein (predicted)	**1.67**	1.07	5.11
361552	Wtip_predicted	WT1-interacting protein (predicted)	**1.65**	−1.04	6.57
89789	Lbr	Lamin B receptor	**−1.64**	−1.15	4.65
306860	Gcnt2	Glucosaminyl (N-acetyl) transferase 2, I-branching enzyme	**−1.69**	−1.05	7.28
64629	Porf1	Preoptic regulatory factor 1	**−1.85**	−1.65	7.41
312316	Doxl1	Diamine oxidase-like protein 1	**−2.53**	1.22	4.48
366624	Cfl2_predicted	Cofilin 2, muscle (predicted)	**−2.83**	1.13	2.71
360949	Cpeb2_predicted	Cytoplasmic polyadenylation element binding protein 2 (predicted)	**−3.61**	1.04	4.48
No data					
307494	RGD1305640 predicted	Similar to RIKEN cD 2410080P20 (predicted)	**2.79**	1.80	3.61
289235	Slamf9_predicted	SLAM family member 9 (predicted)	**2.68**	1.41	4.31
308794	RGD1310371	Similar to RIKEN cD 1700026D08	**2.60**	1.66	6.11
300317	RGD1311154 predicted	Similar to hypothetical protein FLJ12242 (predicted)	**2.35**	1.49	9.42
361267	Akr1cl1_predicted	Aldo-keto reductase family 1, member C-like 1 (predicted)	**2.33**	1.27	4.69
361853	RGD1311294 predicted	Similar to hypothetical protein C6orf60 (predicted)	**2.30**	1.48	5.59
691504	LOC691504	Similar to Zinc finger protein ZFPM1 (Zinc finger protein multitype 1) (friend of GATA protein 1) (friend of GATA-1) (FOG-1)	**2.27**	1.33	6.99
500200	RGD1561512 predicted	Similar to bHLH factor Math6 (predicted)	**2.25**	1.49	3.89
313837	RGD1562284 predicted	Similar to glutaminyl-peptide cyclotransferase precursor (QC) (predicted)	**2.13**	1.67	6.75
499745	LOC499745	Similar to Notch-regulated ankyrin repeat protein	**1.96**	1.20	4.64
266764	Tbkbp1	TBK1 binding protein 1	**1.89**	1.42	6.62
361519	RGD1564862 predicted	Similar to hypothetical protein MGC51082 (predicted)	**1.84**	1.27	8.61
303671	Fads6_predicted	Fatty acid desaturase domain family, member 6 (predicted)	**1.72**	1.18	7.71
362246	Trp53inp2	Tumor protein p53 inducible nuclear protein 2	**1.68**	1.39	9.41
500059	RGD1559885 predicted	Similar to hypothetical gene supported by BC063892 (predicted)	**1.65**	1.09	6.93
117054	Cd52	CD52 antigen	1.59	**6.54**	2.76
691478	LOC691478	Similar to copine-6 (copine VI) (Neuronal-copine) (N-copine)	**−1.71**	−1.39	8.28
305549	Peli1	Pellino homolog 1 (Drosophila)	**−1.71**	1.00	7.21
499839	RGD1564664 predicted	Similar to LOC387763 protein (predicted)	**−1.73**	−1.17	9.48
494538	LOC494538	ABPβ	**−1.78**	−1.24	5.12
691164	LOC691164	Similar to pellino homolog 1 (Drosophila)	**−1.92**	−1.04	7.27
363496	Armcx6	Armadillo repeat containing, X-linked 6	**−1.96**	−1.13	6.91
500204	RGD1562515 predicted	Similar to RIKEN cD 4931417E11 (predicted)	**−1.97**	−1.32	4.32
361003	Dupd1_predicted	Dualspecificity phosphatase and proisomerase domain containing 1 (predicted)	**−2.28**	1.01	2.91
298605	RGD1566169 predicted	Similar to hypothetical protein MGC37938 (predicted)	**−2.50**	−1.60	5.62

Shown are the genes with a fold change above 1.6 or below −1.6, in any of the SD or RD groups. Fold changes are represented in natural scale, computing the magnitude with the most abundant transcript in the numerator. The sign indicates the direction of the change: positive values refer to greater transcript abundance in RD or SD respect to the reference (TX), whereas negative values indicate less abundance. Shown also is the A value: mean of the log2 intensity values over all samples as a measure of the average expression level. The genes are grouped by the BP categories of GO. Repeated probes were not omitted. In *bold*, the fold change of probes with $P_{adjust} < 0.05$. MF, Molecular functions.

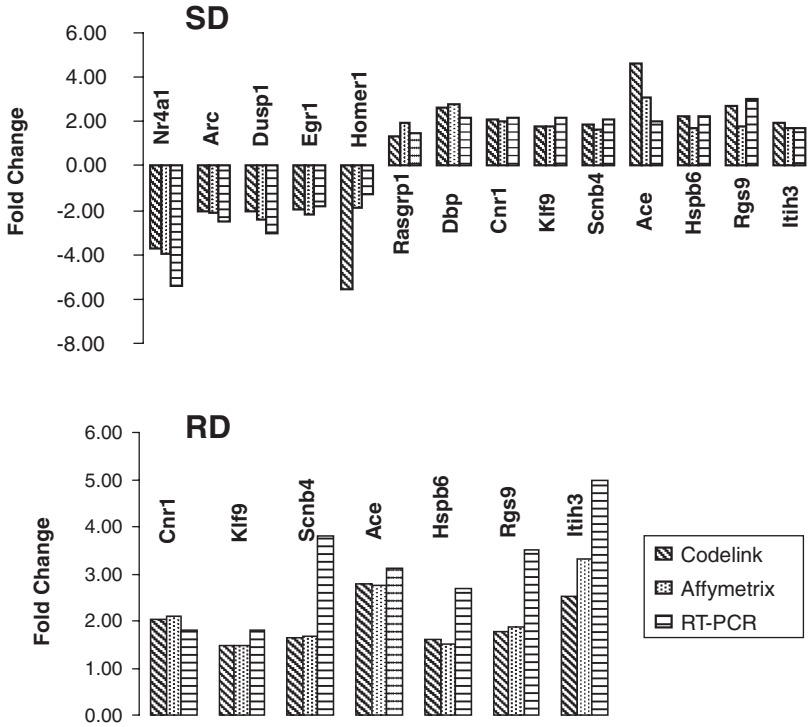

FIG. 3. Correlation between data from Codelink and Affymetrix hybridizations and Taqman PCR assays of selected differentially expressed genes from the SD and RD groups.

From the genes common to both platforms (supplemental Table 5), five were up-regulated by both T_3 treatment schedules (see below), and three were up-regulated by the RD only (*Hba1*, *Alas2*, *Loc287167*). From the SD treatments, 26 up-regulated and 14 down-regulated genes were confirmed in both platforms. Among the SD up-regulated genes, *hr* (or *hairless*), *Rasd2* (also known as Rhes), and *Klf9* (also known as BTEB) are already known to be thyroid hormone-regulated genes. Among the SD down-regulated genes, there were several early response genes (*Egr1*, *Arc*, *Dusp1*, *Egr4*, *Fos*, *Nr4a1*, *Nr4a3*, *Egr2*, and *Homer1*).

For biological confirmation using Taqman PCR, we used a different group of rats from the ones used for the arrays. The genes selected for confirmation included the five genes that were up-regulated by both SD and RD in both platforms: *Ace* (angiotensin converting enzyme), *Hspb6* (heat shock protein B6), *Cnr1* (cannabinoid receptor 1), *Itih3* (inter-α trypsin inhibitor), and *Scn4b* (voltage-gated sodium channel IV). We also checked *Rgs9* (regulator of G protein signaling 9), a striatum-specific gene (47), which shows a robust increase by SD; *Klf9* (Kruppel-like factor, also known as basic transcription factor binding protein, or BTEB), a gene previously shown to be regulated by thyroid hormone in several cell types (48); *Dbp* (D-site binding protein); *Rasgrp1* (also known as CalDAG-GEF1); and the early response genes *Nr4a1*(also known as NGFIB), *Arc*, *Dusp1*, *Egr1* (also known as NGFIA), and *Homer1*. The results, shown in Fig. 3, show that there was a good correlation between the results from the arrays and the PCR, both in the direction and magnitude of expression changes.

Discussion

In this article we provide, for the first time, a comprehensive list of genes that are differentially expressed by thyroid hormone in the adult striatum. Our approach involved the analysis of gene expression after administration of T_3 to hypothyroid rats.

Most previous studies on the effects of T_3 on brain gene expression have been limited to the postnatal period, and few genes were known to be sensitive to T_3 in the adult brain. In one study, Haas *et al.* (49) used a limited set of 1224 neural-specific genes and found that hyperthyroidism induced only modest changes in the expression of 11 genes. This study is not comparable with ours, first because of the limited number of genes in the array, second because total brain was analyzed, and third because T_3 was given at doses 10-fold higher than in this work and for 10 consecutive days so that the animals were hyperthyroid.

One of the earliest genes identified as regulated by T_3 in the adult brain is *Nrgn*, a gene confirmed to be regulated at the transcriptional level in cultured neurons (50) and demonstrated to be a sensitive marker of T_3 action. *Nrgn* was not recovered initially in the list of candidate genes because it was not present as a hybridizable probe in the arrays. However, it was present in the Affymetrix chips and was detected after the acute and multiple-dose treatments, in agreement with previous studies. Other genes present as candidate genes and previously shown to be regulated by thyroid hormones in other paradigms include *Klf9* (48), *Egr1* (51), the mitochondrial importer *Tomm70* (52), the transcription factor *Hr* (53), the small G protein *Rasd2* (also known as Rhes) (54), the transcription factor *Nr4a1* (55), the cannabinoid receptor *Cnr1* (31), and the dual-specificity phosphatase *Dusp1* (56).

Early studies by Oppenheimer and colleagues (57) showed that the response of some genes, such as pituitary GH, followed a linear response in relation to nuclear occupancy after T_3 administration. Expression of these genes did not increase above the baseline euthyroid level. For other genes, exem-

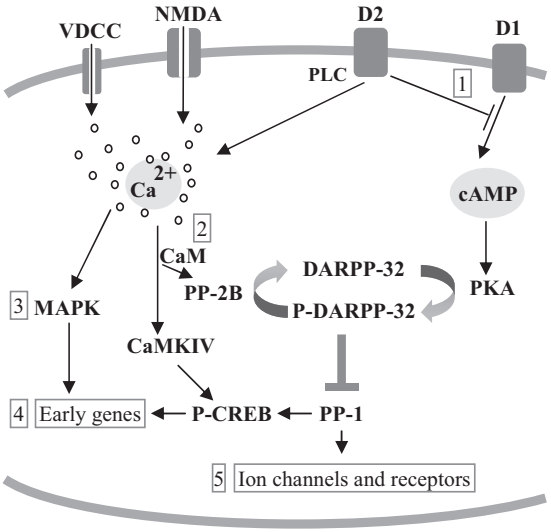

FIG. 4. Role of thyroid hormone in the control of signaling in the striatum. Shown is a simplified scheme of signaling pathways in the striatum. DARPP-32 phosphorylation is under control of the cAMP pathway, which promotes phosphorylation, and by the Ca^{2+}-calmodulin (CaM) pathway, which promotes dephosphorylation. cAMP production is under control of G protein-coupled membrane receptors such as dopamine receptors (D1, D2) and others not included in the figure, such as opiate receptors, adenosine, and serotonin receptors. Voltage-dependent Ca2+ channels (VDCC), *N*-methyl-D-aspartate (NMDA) glutamate receptors, dopamine 2 receptors (D2), and $GABA_A$ receptors (not shown) regulate intracellular Ca^{2+} concentration and CaM activation. Genes regulated by thyroid hormone are involved in different control points of the signaling cascade, as shown by the *arabic numerals*: 1, G protein-coupled receptors; 2, Ca2+ signaling and CaM activation; 3, MAPK pathways; 4, early gene transcription; 5, ion channels. PLC, Phospholipase C; PKA, protein kinase A; PP-2B, calcium and calmodulin-dependent protein phosphatase, or calcineurin; CaMKIV, calcium and calmodulin-dependent kinase IV; PP-1, protein phosphatase 1.

plified by liver enzymes, the response was nonlinear and amplified with further increases of receptor occupancy above the euthyroid level of about 50% (12).

Based on these studies, the dosage and timing of T_3 administration was chosen by us so that two different situations were reached. The single dose was intended to result in near full saturation of nuclear receptors for 24 h. Twenty-four hours after injection, the fractional occupancy of nuclear receptors was calculated to be 0.86. In the case of multiple injections, the fractional occupancy 24 h after the last injection was 0.49, which is the physiological occupancy of T_3 receptors in liver (12). The single injection protocol should likely select for fast, linear, and amplified responses after T_3, whereas the multiple injection dosage should identify linear, steady-state responses. Therefore, it is not surprising that the number of candidate genes was larger after the acute injection of T_3 than after the multiple daily doses. In the RD group, there were one down-regulated gene and eight up-regulated genes. The only down-regulated gene, *Gja7*, encodes a gap junction membrane channel protein expressed in several regions of the central nervous system but not in the striatum (58). This agrees with the almost no expression found in the RD-treated rats, indicating that thyroid hormone is involved in maintaining *Gja7* repression under normal conditions. Three of the up-regulated genes were of red blood cell origin. The significance of this finding is uncertain. Interestingly, *Hba1* has also been found previously to be regulated by T_3 in the cerebellum *in vivo* and in primary cultures of cerebellar granular cells, presumably at the transcriptional level (56). The functional significance of the regulation of the rest of genes comprising this small set of candidate genes is uncertain because they do not share common functional properties.

Despite the above, the expression of many genes after the RD falls between the levels of the hypothyroid and acutely treated rats, indicating that the group of genes sensitive to each of the treatment schedules is qualitatively similar. Actually, we calculate that 52% of the differentially expressed genes in the SD were changed in the RD by at least 20%, and in the same direction. This justifies the functional analysis performed using the PANTHER resource from the list of all candidate genes found under the two treatment schedules. On the other hand, the overlap between the SD and RD suggests that the genes induced in both treatment schedules are regulated at the transcriptional level.

PANTHER analysis of the significance of represented pathways disclosed three genes of the circadian clock system. Although not present in the PANTHER analysis, another regulated gene, *Dbp*, has been described as a circadian gene (59). Also, other genes related to the wakefulness (*Fos*, *Arc*, *Hsps*, *Egr1*, *Homer*) (59) were sensitive to T_3. Because at least one of these genes, *Dbp*, has been proposed as a candidate gene in bipolar disorders (60), it is tempting to speculate that the beneficial effects of large doses of thyroid hormones in bipolar disorders is mediated, at least in part, through regulation of the expression of these genes.

Another group of candidate genes have important roles in the physiology of striatal neurons. There are 314 genes of enriched expression in the striatum (61), from which 21 were differentially expressed after T_3 treatment (supplemental Table 6). Some of these genes are defective in Huntington's disease (37), such as *Scn4b*, *Rasd2*, *Rasgrp1*, *Klf9*, *and Rgs9*. The latter is also one of the 10 most enriched genes in the striatum in relation to other brain regions (61). Central to striatal neuron signaling is the regulation of dopamine and cAMP-regulated phosphoprotein (DARPP)-32 phosphorylation [Fig 4 (62)]. Phospho-DARPP-32 levels are controlled by the cAMP-protein kinase A pathway, which promotes phosphorylation, and by the Ca^{2+}-calcineurin pathway, which promotes dephosphorylation. *Rgs9* and *Rasd2* are involved in G protein signaling regulating the cAMP pathway (47, 63), whereas *Nrgn* is involved in the regulation of the Ca^{2+}/calmodulin pathway (64). In addition, sodium channels and some of the early response genes, such as *Arc*, *Homer*, and *Dusp1*, are also regulated by phospho-DARPP-32. A large fraction of the candidate genes found in the screening are also involved in intracellular signaling cascades involving G protein and cation transport. Therefore, thyroid hormone is involved in maintaining an optimal signaling in the striatum by acting at multiple control points.

In conclusion, we have identified for the first time a set of genes whose expression is dependent on thyroid hormone in the adult striatum. We believe that this work opens the way for more detailed analysis of the effects of thyroid hormone

in the adult brain and their beneficial therapeutic effects in affective disorders.

Acknowledgments

The technical expertise of Eulalia Moreno and Ana Torrecilla is gratefully acknowledged.

Received March 13, 2008. Accepted April 30, 2008.

Address all correspondence and requests for reprints to: Beatriz Morte and Juan Bernal, Instituto de Investigaciones Biomédicas, Arturo Duperier 4, 28029 Madrid, Spain. E-mail: bmorte@iib.uam.es; or jbernal@iib.uam.es.

This work was supported by Grant BFU2005-01740 from the Ministry of Education and Science of Spain, the European Union Integrated Project CRESCENDO (Consortium for Research on Nuclear Receptors in Development and Aging) Grant LSHM-CT-2005-018652, and the Centro de Investigación Biomédica en Red de Enfermedades Raras, Instituto de Salud Carlos III.

Present address for D.D.: Bioinformatics Center, Institute for Chemical Research, Kyoto University, Uji, Kyoto 6110011, Japan.

Disclosure Statement: The authors have nothing to disclose.

References

1. **Oppenheimer JH, Schwartz HL** 1997 Molecular basis of thyroid hormone-dependent brain development. Endocr Rev 18:462–475
2. **Bernal J** 2005 Thyroid hormones and brain development. Vitam Horm 71: 95–122
3. **Bernal J** 2007 Thyroid hormone receptors in brain development and function. Nat Clin Pract Endocrinol Metab 3:249–259
4. **Simon NM, Blacker D, Korbly NB, Sharma SG, Worthington JJ, Otto MW, Pollack MH** 2002 Hypothyroidism and hyperthyroidism in anxiety disorders revisited: new data and literature review. J Affect Disord 69:209–217
5. **Baumgartner A, Bauer M, Hellweg R** 1994 Treatment of intractable non-rapid cycling bipolar affective disorder with high-dose thyroxine: an open clinical trial. Neuropsychopharmacology 10:183–189
6. **Bauer M, London ED, Rasgon N, Berman SM, Frye MA, Altshuler LL, Mandelkern MA, Bramen J, Voytek B, Woods R, Mazziotta JC, Whybrow PC** 2005 Supraphysiological doses of levothyroxine alter regional cerebral metabolism and improve mood in bipolar depression. Mol Psychiatry 10:456–469
7. **Bauer M, Heinz A, Whybrow PC** 2002 Thyroid hormones, serotonin and mood: of synergy and significance in the adult brain. Mol Psychiatry 7:140–156
8. **Lemkine GF, Raj A, Alfama G, Turque N, Hassani Z, Alegria-Prevot O, Samarut J, Levi G, Demeneix BA** 2005 Adult neural stem cell cycling *in vivo* requires thyroid hormone and its α receptor. FASEB J 19:863–865
9. **Montero-Pedrazuela A, Venero C, Lavado-Autric R, Fernandez-Lamo I, Garcia-Verdugo JM, Bernal J, Guadano-Ferraz A** 2006 Modulation of adult hippocampal neurogenesis by thyroid hormones: implications in depressive-like behavior. Mol Psychiatry 11:361–371
10. **Venero C, Guadano-Ferraz A, Herrero AI, Nordstrom K, Manzano J, de Escobar GM, Bernal J, Vennstrom B** 2005 Anxiety, memory impairment, and locomotor dysfunction caused by a mutant thyroid hormone receptor α1 can be ameliorated by T_3 treatment. Genes Dev 19:2152–2163
11. **Iñiguez MA, Rodriguez-Pena A, Ibarrola N, Morreale de Escobar G, Bernal J** 1992 Adult rat brain is sensitive to thyroid hormone. Regulation of RC3/neurogranin mRNA. J Clin Invest 90:554–558
12. **Oppenheimer JH, Coulombe P, Schwartz HL, Gutfeld NW** 1978 Nonlinear (amplified) relationship between nuclear occupancy by triiodothyronine and the appearance rate of hepatic α-glycerophosphate dehydrogenase and malic enzyme in the rat. J Clin Invest 61:987–997
13. **Escobar-Morreale HF, del Rey FE, Obregon MJ, de Escobar GM** 1996 Only the combined treatment with thyroxine and triiodothyronine ensures euthyroidism in all tissues of the thyroidectomized rat. Endocrinology 137: 2490–2502
14. **Goumaz MO, Schwartz H, Oppenheimer JH, Mariash CN** 1994 Kinetic model of the response of precursor and mature rat hepatic mRNA-S14 to thyroid hormone. American J Physiol 266:E1001–E1011
15. **Zavacki AM, Ying H, Christoffolete MA, Aerts G, So E, Harney JW, Cheng SY, Larsen PR, Bianco AC** 2005 Type 1 iodothyronine deiodinase is a sensitive marker of peripheral thyroid status in the mouse. Endocrinology 146: 1568–1575
16. **Livak KJ, Schmittgen TD** 2001 Analysis of relative gene expression data using real-time quantitative PCR and the 2[-ΔΔC(T)] method. Methods (San Diego) 25:402–408
17. **Team RDC** 2005 R: a language and environment for statistical computing. Vienna, Austria: R Foundation for Statistical Computing
18. **Carey VJ, Gentry J, Whalen E, Gentleman R** 2005 Network structures and algorithms in Bioconductor. Bioinformatics 21:135–136
19. **Gentleman RC, Carey VJ, Bates DM, Bolstad B, Dettling M, Dudoit S, Ellis B, Gautier L, Ge Y, Gentry J, Hornik K, Hothorn T, Huber W, Iacus S, Irizarry R, Leisch F, Li C, Maechler M, Rossini AJ, Sawitzki G, Smith C, Smyth G, Tierney L, Yang JY, Zhang J** 2004 Bioconductor: open software development for computational biology and bioinformatics. Genome Biol 5:R80
20. **Diez D, Alvarez R, Dopazo A** 2007 Codelink: an R package for analysis of GE healthcare gene expression bioarrays. Bioinformatics 23:1168–1169
21. **Irizarry R, Gautier L, Bolstad B, Miller C, Astrand M, Cope LM, Gentleman R, Gentry J, Halling C, Huber W, MacDonald J, Rubinstein B, Workman C, Zhang J** 2006 Affy: methods for Affymetrix oligonucleotide arrays. Available at http://bioconductor.org/packages/2.2/bioc/html/affy.html
22. **Gentleman R, Carey V, Huber W, FH** 2007 Genefilter: methods for filtering genes from microarray experiments. Available at http://bioconductor.org/packages/2.2/bioc/html/genefilter.html
23. **Smyth GK, Michaud J, Scott HS** 2005 Use of within-array replicate spots for assessing differential expression in microarray experiments. Bioinformatics 21:2067–2075
24. **Hochberg Y, Benjamini Y** 1990 More powerful procedures for multiple significance testing. Stat Med 9:811–818
25. **Irizarry RA, Hobbs B, Collin F, Beazer-Barclay YD, Antonellis KJ, Scherf U, Speed TP** 2003 Exploration, normalization, and summaries of high density oligonucleotide array probe level data. Biostatistics 4:249–264
26. **Ashburner M, Ball CA, Blake JA, Botstein D, Butler H, Cherry JM, Davis AP, Dolinski K, Dwight SS, Eppig JT, Harris MA, Hill DP, Issel-Tarver L, Kasarskis A, Lewis S, Matese JC, Richardson JE, Ringwald M, Rubin GM, Sherlock G** 2000 Gene ontology: tool for the unification of biology. The Gene Ontology Consortium. Nat Genet 25:25–29
27. **Thomas PD, Campbell MJ, Kejariwal A, Mi H, Karlak B, Daverman R, Diemer K, Muruganujan A, Narechania A** 2003 PANTHER: a library of protein families and subfamilies indexed by function. Genome Res 13:2129–2141
28. **Cleveland WS, Grosse E, Shyu WM** 1992 Statistical models in S. Chambers J, Hastie T, eds. Dordrecht: The Netherlands: Chapman and Hall, Kluwer Academic Publishers; 309–376
29. **Sohl G, Maxeiner S, Willecke K** 2005 Expression and functions of neuronal gap junctions. Nat Rev Neurosci 6:191–200
30. **Brotchie JM** 2003 CB1 cannabinoid receptor signalling in Parkinson's disease. Curr Opin Pharmacol 3:54–61
31. **Asua T, Bilbao A, Gorriti MA, Lopez JA, Del Mar Alvarez M, Navarro M, de Fonseca FR, Perez-Castillo A, Santos A** 2008 Implication of the endocannabinoid system in the locomotor hyperactivity associated with congenital hypothyroidism. Endocrinology 149:2657–2666
32. **von Bohlen und Halbach O** 2005 The renin-angiotensin system in the mammalian central nervous system. Curr Protein Pept Sci 6:355–371
33. **Suwelack D, Hurtado-Lorenzo A, Millan E, Gonzalez-Nicolini V, Wawrowsky K, Lowenstein PR, Castro MG** 2004 Neuronal expression of the transcription factor Gli1 using the Tα1α-tubulin promoter is neuroprotective in an experimental model of Parkinson's disease. Gene Ther 11:1742–1752
34. **Kato M, Seki N, Sugano S, Hashimoto K, Masuho Y, Muramatsu M, Kaibuchi K, Nakafuku M** 2001 Identification of sonic hedgehog-responsive genes using cDNA microarray. Biochem Biophys Res Commun 289:472–478
35. **Eisenhofer G** 2001 The role of neuronal and extraneuronal plasma membrane transporters in the inactivation of peripheral catecholamines. Pharmacol Ther 91:35–62
36. **Wong HK, Sakurai T, Oyama F, Kaneko K, Wada K, Miyazaki H, Kurosawa M, De Strooper B, Saftig P, Nukina N** 2005 β Subunits of voltage-gated sodium channels are novel substrates of β-site amyloid precursor protein-cleaving enzyme (BACE1) and γ-secretase. J Biol Chem 280:23009–23017
37. **Desplats PA, Kass KE, Gilmartin T, Stanwood GD, Woodward EL, Head SR, Sutcliffe JG, Thomas EA** 2006 Selective deficits in the expression of striatal-enriched mRNAs in Huntington's disease. J Neurochem 96:743–757
38. **Quraishe S, Asuni A, Boelens WC, O'Connor V, Wyttenbach A** 2008 Expression of the small heat shock protein family in the mouse CNS: differential anatomical and biochemical compartmentalization. Neuroscience 153:483–491
39. **Ogden AT, Nunes I, Ko K, Wu S, Hines CS, Wang AF, Hegde RS, Lang RA** 1998 GRIFIN, a novel lens-specific protein related to the galactin family. J Biol Chem 273:28889–28896
40. **Kuespert K, Pils S, Hauck CR** 2006 CEACAMs: their role in physiology and pathophysiology. Curr Opin Cell Biol 18:565–571
41. **Helfand BT, Mendez MG, Pugh J, Delsert C, Goldman RD** 2003 A role for intermediate filaments in determining and maintaining the shape of nerve cells. Molecular Biol Cell 14:5069–5081
42. **Konishi H, Namikawa K, Shikata K, Kobatake Y, Tachibana T, Kiyama H** 2007 Identification of peripherin as a Akt substrate in neurons. J Biol Chem 282:23491–23499
43. **Guo L, Lobenhofer EK, Wang C, Shippy R, Harris SC, Zhang L, Mei N, Chen T, Herman D, Goodsaid FM, Hurban P, Phillips KL, Xu J, Deng X, Sun YA, Tong W, Dragan YP, Shi L** 2006 Rat toxicogenomic study reveals analytical consistency across microarray platforms. Nat Biotechnol 24:1162–1169
44. **Shi L, Tong W, Fang H, Scherf U, Han J, Puri RK, Frueh FW, Goodsaid FM, Guo L, Su Z, Han T, Fuscoe JC, Xu ZA, Patterson TA, Hong H, Xie Q, Perkins**

RG, Chen JJ, Casciano DA 2005 Cross-platform comparability of microarray technology: intra-platform consistency and appropriate data analysis procedures are essential. BMC Bioinformatics 6(Suppl 2):S12
45. **Shi L, Reid LH, Jones WD, Shippy R, Warrington JA, Baker SC, Collins PJ, de Longueville F, Kawasaki ES, Lee KY, Luo Y, Sun YA, Willey JC, Setterquist RA, Fischer GM, Tong W, Dragan YP, Dix DJ, Frueh FW, Goodsaid FM, Herman D, Jensen RV, Johnson CD, Lobenhofer EK, Puri RK,** *et al.* 2006 The MicroArray Quality Control (MAQC) project shows inter- and intraplatform reproducibility of gene expression measurements. Nat Biotechnol 24:1151–1161
46. **Koritschoner NP, Alvarez-Dolado M, Kurz SM, Heikenwalder MF, Hacker C, Vogel F, Munoz A, Zenke M** 2001 Thyroid hormone regulates the obesity gene tub. EMBO Rep 2:499–504
47. **Thomas EA, Danielson PE, Sutcliffe JG** 1998 RGS9: a regulator of G-protein signalling with specific expression in rat and mouse striatum. J Neurosci Res 52:118–124
48. **Denver RJ, Ouellet L, Furling D, Kobayashi A, Fujii-Kuriyama Y, Puymirat J** 1999 Basic transcription element-binding protein (BTEB) is a thyroid hormone-regulated gene in the developing central nervous system. Evidence for a role in neurite outgrowth. J Biol Chem 274:23128–23134
49. **Haas MJ, Mreyoud A, Fishman M, Mooradian AD** 2004 Microarray analysis of thyroid hormone-induced changes in mRNA expression in the adult rat brain. Neurosci Lett 365:14–18
50. **Morte B, Iñiguez MA, Lorenzo PI, Bernal J** 1997 Thyroid hormone-regulated expression of RC3/neurogranin in the immortalized hypothalamic cell line GT1–7. J Neurochem 69:902–909
51. **Pipaon C, Santos A, Perez-Castillo A** 1992 Thyroid hormone up-regulates NGFI-A gene expression in rat brain during development. J Biol Chem 267:21–23
52. **Alvarez-Dolado M, Gonzalez-Moreno M, Valencia A, Zenke M, Bernal J, Munoz A** 1999 Identification of a mammalian homologue of the fungal Tom70 mitochondrial precursor protein import receptor as a thyroid hormone-regulated gene in specific brain regions. J Neurochem 73:2240–2249
53. **Thompson CC** 1996 Thyroid hormone-responsive genes in developing cerebellum include a novel synaptotagmin and a hairless homolog. J Neurosci 16:7832–7840
54. **Vargiu P, Morte B, Manzano J, Perez J, de Abajo R, Gregor Sutcliffe J, Bernal J** 2001 Thyroid hormone regulation of rhes, a novel Ras homolog gene expressed in the striatum. Brain Res Mol Brain Res 94:1–8
55. **Dong H, Yauk CL, Williams A, Lee A, Douglas GR, Wade MG** 2007 Hepatic gene expression changes in hypothyroid juvenile mice: characterization of a novel negative thyroid-responsive element. Endocrinology 148:3932–3940
56. **Quignodon L, Grijota-Martinez C, Compe E, Guyot R, Allioli N, Laperriere D, Walker R, Meltzer P, Mader S, Samarut J, Flamant F** 2007 A combined approach identifies a limited number of new thyroid hormone target genes in post-natal mouse cerebellum. J Mol Endocrinol 39:17–28
57. **Coulombe P, Schwartz HL, Oppenheimer JH** 1978 Relationship between the accumulation of pituitary growth hormone and nuclear occupancy by triiodothyronine in the rat. J Clin Invest 62:1020–1028
58. **Maxeiner S, Krüger O, Schilling K, Traub O, Urschel S, Willecke K** 2003 Spatiotemporal transcription of connexin45 during brain development results in neuronal expression in adult mice. Neuroscience 119:689–700
59. **Cirelli C, Gutierrez CM, Tononi G** 2004 Extensive and divergent effects of sleep and wakefulness on brain gene expression. Neuron 41:35–43
60. **Niculescu 3rd AB, Segal DS, Kuczenski R, Barrett T, Hauger RL, Kelsoe JR** 2000 Identifying a series of candidate genes for mania and psychosis: a convergent functional genomics approach. Physiol Genomics 4:83–91
61. **Stansberg C, Vik-Mo AO, Holdhus R, Breilid H, Srebro B, Petersen K, Jorgensen HA, Jonassen I, Steen VM** 2007 Gene expression profiles in rat brain disclose CNS signature genes and regional patterns of functional specialisation. BMC Genomics 8:94
62. **Greengard P** 2001 The neurobiology of slow synaptic transmission. Science 294:1024–1030
63. **Vargiu P, De Abajo R, Garcia-Ranea JA, Valencia A, Santisteban P, Crespo P, Bernal J** 2004 The small GTP-binding protein, Rhes, regulates signal transduction from G protein-coupled receptors. Oncogene 23:559–568
64. **Gerendasy DD, Sutcliffe JG** 1997 RC3/neurogranin, a postsynaptic calpacitin for setting the response threshold to calcium influxes. Mol Neurobiol 15:131–163

***Endocrinology* is published monthly by The Endocrine Society (http://www.endo-society.org), the foremost professional society serving the endocrine community.**